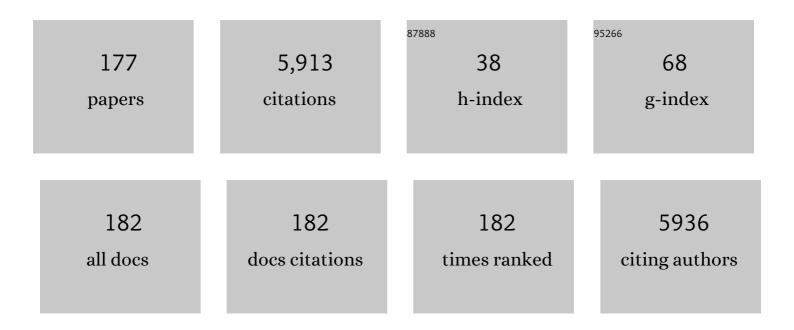
Krishna S Nayak

List of Publications by Year in descending order

Source: https://exaly.com/author-pdf/351930/publications.pdf Version: 2024-02-01



KDISHNA S NAVAK

#	Article	IF	CITATIONS
1	kâ€ŧ FOCUSS: A general compressed sensing framework for high resolution dynamic MRI. Magnetic Resonance in Medicine, 2009, 61, 103-116.	3.0	536
2	Saturated double-angle method for rapidB1+ mapping. Magnetic Resonance in Medicine, 2006, 55, 1326-1333.	3.0	297
3	An approach to real-time magnetic resonance imaging for speech production. Journal of the Acoustical Society of America, 2004, 115, 1771-1776.	1.1	256
4	Myocardial first-pass perfusion cardiovascular magnetic resonance: history, theory, and current state of the art. Journal of Cardiovascular Magnetic Resonance, 2008, 10, 18.	3.3	185
5	Cardiovascular magnetic resonance phase contrast imaging. Journal of Cardiovascular Magnetic Resonance, 2015, 17, 71.	3.3	184
6	Comparison of Fat–Water MRI and Singleâ€voxel MRS in the Assessment of Hepatic and Pancreatic Fat Fractions in Humans. Obesity, 2010, 18, 841-847.	3.0	182
7	Identification of brown adipose tissue in mice with fat–water IDEALâ€MRI. Journal of Magnetic Resonance Imaging, 2010, 31, 1195-1202.	3.4	131
8	Real-time magnetic resonance imaging and electromagnetic articulography database for speech production research (TC). Journal of the Acoustical Society of America, 2014, 136, 1307-1311.	1.1	120
9	Assessment of abdominal adipose tissue and organ fat content by magnetic resonance imaging. Obesity Reviews, 2011, 12, e504-15.	6.5	112
10	Ethnic Differences in Pancreatic Fat Accumulation and Its Relationship With Other Fat Depots and Inflammatory Markers. Diabetes Care, 2011, 34, 485-490.	8.6	112
11	Real-time color flow MRI. Magnetic Resonance in Medicine, 2000, 43, 251-258.	3.0	105
12	Synchronized and noise-robust audio recordings during realtime magnetic resonance imaging scans. Journal of the Acoustical Society of America, 2006, 120, 1791-1794.	1.1	104
13	MR properties of brown and white adipose tissues. Journal of Magnetic Resonance Imaging, 2011, 34, 468-473.	3.4	104
14	Fat-suppressed steady-state free precession imaging using phase detection. Magnetic Resonance in Medicine, 2003, 50, 210-213.	3.0	101
15	Real-time cardiac MRI at 3 tesla. Magnetic Resonance in Medicine, 2004, 51, 655-660.	3.0	101
16	Designing long-T2 suppression pulses for ultrashort echo time imaging. Magnetic Resonance in Medicine, 2006, 56, 94-103.	3.0	85
17	Recommendations for real-time speech MRI. Journal of Magnetic Resonance Imaging, 2016, 43, 28-44.	3.4	84
18	Seeing speech: Capturing vocal tract shaping using real-time magnetic resonance imaging [Exploratory DSP]. IEEE Signal Processing Magazine, 2008, 25, 123-132.	5.6	82

#	Article	IF	CITATIONS
19	Clinical Image Quality Assessment of Accelerated Magnetic Resonance Neuroimaging Using Compressed Sensing. Investigative Radiology, 2013, 48, 638-645.	6.2	81
20	MRI artifacts and correction strategies. Imaging in Medicine, 2010, 2, 445-457.	0.0	69
21	Differential Computed Tomographic Attenuation of Metabolically Active and Inactive Adipose Tissues. Journal of Computer Assisted Tomography, 2011, 35, 65-71.	0.9	66
22	Accelerated threeâ€dimensional upper airway MRI using compressed sensing. Magnetic Resonance in Medicine, 2009, 61, 1434-1440.	3.0	63
23	Assessment of myocardial blood flow (MBF) in humans using arterial spin labeling (ASL): Feasibility and noise analysis. Magnetic Resonance in Medicine, 2009, 62, 975-983.	3.0	61
24	Spiral balanced steadyâ€state free precession cardiac imaging. Magnetic Resonance in Medicine, 2005, 53, 1468-1473.	3.0	60
25	Measurement and characterization of RF nonuniformity over the heart at 3T using body coil transmission. Journal of Magnetic Resonance Imaging, 2008, 27, 643-648.	3.4	59
26	Wideband SSFP: Alternating repetition time balanced steady state free precession with increased band spacing. Magnetic Resonance in Medicine, 2007, 58, 931-938.	3.0	58
27	Computational fluid dynamics simulations of blood flow regularized by 3D phase contrast MRI. BioMedical Engineering OnLine, 2015, 14, 110.	2.7	56
28	A fast and flexible MRI system for the study of dynamic vocal tract shaping. Magnetic Resonance in Medicine, 2017, 77, 112-125.	3.0	53
29	Three dimensional first-pass myocardial perfusion imaging at 3T: feasibility study. Journal of Cardiovascular Magnetic Resonance, 2008, 10, 57.	3.3	50
30	Ectopic Fat Deposition in Prediabetic Overweight and Obese Minority Adolescents. Journal of Clinical Endocrinology and Metabolism, 2013, 98, 1115-1121.	3.6	50
31	Arterial Spin Labeled CMR Detects Clinically Relevant Increase in Myocardial Blood Flow With Vasodilation. JACC: Cardiovascular Imaging, 2011, 4, 1253-1261.	5.3	48
32	Real-time imaging of skeletal muscle velocity. Journal of Magnetic Resonance Imaging, 2003, 18, 734-739.	3.4	47
33	Flexible retrospective selection of temporal resolution in real-time speech MRI using a golden-ratio spiral view order. Magnetic Resonance in Medicine, 2011, 65, 1365-1371.	3.0	47
34	Rapid quantitation of high-speed flow jets. Magnetic Resonance in Medicine, 2003, 50, 366-372.	3.0	46
35	Paralinguistic mechanisms of production in human "beatboxing― A real-time magnetic resonance imaging study. Journal of the Acoustical Society of America, 2013, 133, 1043-1054.	1.1	46
36	Accelerated cardiac cine MRI using locally low rank and finite difference constraints. Magnetic Resonance Imaging, 2016, 34, 707-714.	1.8	43

#	Article	IF	CITATIONS
37	Myocardial arterial spin labeling. Journal of Cardiovascular Magnetic Resonance, 2016, 18, 22.	3.3	43
38	Direct estimation of tracerâ€kinetic parameter maps from highly undersampled brain dynamic contrast enhanced MRI. Magnetic Resonance in Medicine, 2017, 78, 1566-1578.	3.0	42
39	Threeâ€dimensional firstâ€pass myocardial perfusion MRI using a stackâ€ofâ€spirals acquisition. Magnetic Resonance in Medicine, 2013, 69, 839-844.	3.0	38
40	Automatic intraâ€subject registrationâ€based segmentation of abdominal fat from water–fat MRI. Journal of Magnetic Resonance Imaging, 2013, 37, 423-430.	3.4	38
41	Noninvasive identification and assessment of functional brown adipose tissue in rodents using hyperpolarized 13C imaging. International Journal of Obesity, 2014, 38, 126-131.	3.4	38
42	Dynamic 3-D MR Visualization and Detection of Upper Airway Obstruction During Sleep Using Region-Growing Segmentation. IEEE Transactions on Biomedical Engineering, 2016, 63, 431-437.	4.2	38
43	Analysis of speech production real-time MRI. Computer Speech and Language, 2018, 52, 1-22.	4.3	36
44	Soft-Tissue Deformation for In Vivo Volume Animation. , 2007, , .		35
45	Change in the proton <i>T</i> ₁ of fat and water in mixture. Magnetic Resonance in Medicine, 2010, 63, 494-501.	3.0	35
46	Realâ€ŧime 3D magnetic resonance imaging of the pharyngeal airway in sleep apnea. Magnetic Resonance in Medicine, 2014, 71, 1501-1510.	3.0	35
47	Realâ€∓ime Magnetic Resonance Imaging. Journal of Magnetic Resonance Imaging, 2022, 55, 81-99.	3.4	35
48	Real-time interactive coronary MRA. Magnetic Resonance in Medicine, 2001, 46, 430-435.	3.0	33
49	Highly accelerated dynamic contrast enhanced imaging. Magnetic Resonance in Medicine, 2014, 71, 635-644.	3.0	33
50	Single-breathhold, four-dimensional, quantitative assessment of LV and RV function using triggered, real-time, steady-state free precession MRI in heart failure patients. Journal of Magnetic Resonance Imaging, 2005, 22, 59-66.	3.4	32
51	Automatic correction of echoâ€planar imaging (EPI) ghosting artifacts in realâ€time interactive cardiac MRI using sensitivity encoding. Journal of Magnetic Resonance Imaging, 2008, 27, 239-245.	3.4	32
52	Automatic field map generation and off-resonance correction for projection reconstruction imaging. Magnetic Resonance in Medicine, 2000, 43, 151-154.	3.0	31
53	Dynamic 3-D Visualization of Vocal Tract Shaping During Speech. IEEE Transactions on Medical Imaging, 2013, 32, 838-848.	8.9	31
54	Efficient off-resonance correction for spiral imaging. Magnetic Resonance in Medicine, 2001, 45, 521-524.	3.0	30

#	Article	IF	CITATIONS
55	Feasibility of in vivo measurement of carotid wall shear rate using spiral fourier velocity encoded MRI. Magnetic Resonance in Medicine, 2010, 63, 1537-1547.	3.0	30
56	GOCART: GOlden-angle CArtesian randomized time-resolved 3D MRI. Magnetic Resonance Imaging, 2016, 34, 940-950.	1.8	30
57	Improved Glioma Grading Using Deep Convolutional Neural Networks. American Journal of Neuroradiology, 2021, 42, 233-239.	2.4	29
58	Design and use of tailored hardâ€pulse trains for uniformed saturation of myocardium at 3 Tesla. Magnetic Resonance in Medicine, 2008, 60, 997-1002.	3.0	28
59	Accelerated water–fat imaging using restricted subspace field map estimation and compressed sensing. Magnetic Resonance in Medicine, 2012, 67, 650-659.	3.0	28
60	High-resolution whole-brain DCE-MRI using constrained reconstruction: Prospective clinical evaluation in brain tumor patients. Medical Physics, 2016, 43, 2013-2023.	3.0	28
61	Improved imaging of lingual articulation using realâ€time multislice MRI. Journal of Magnetic Resonance Imaging, 2012, 35, 943-948.	3.4	27
62	Impact of Gastric Banding Versus Metformin on β-Cell Function in Adults With Impaired Glucose Tolerance or Mild Type 2 Diabetes. Diabetes Care, 2018, 41, 2544-2551.	8.6	27
63	Velocityâ€selective arterial spin labeling perfusion MRI: A review of the state of the art and recommendations for clinical implementation. Magnetic Resonance in Medicine, 2022, 88, 1528-1547.	3.0	27
64	The future of real-time cardiac magnetic resonance imaging. Current Cardiology Reports, 2005, 7, 45-51.	2.9	26
65	3D dynamic MRI of the vocal tract during natural speech. Magnetic Resonance in Medicine, 2019, 81, 1511-1520.	3.0	26
66	Quantification of absolute fat mass using an adipose tissue reference signal model. Journal of Magnetic Resonance Imaging, 2008, 28, 1483-1491.	3.4	25
67	Evaluation of Swallow Function After Tongue Cancer Treatment Using Real-Time Magnetic Resonance Imaging. JAMA Otolaryngology - Head and Neck Surgery, 2013, 139, 1312.	2.2	25
68	In Vivo Real-Time Intravascular MRI. Journal of Cardiovascular Magnetic Resonance, 2002, 4, 223-232.	3.3	24
69	Myocardial arterial spin labeling perfusion imaging with improved sensitivity. Journal of Cardiovascular Magnetic Resonance, 2014, 16, 15.	3.3	24
70	Dynamic offâ€resonance correction for spiral realâ€time MRI of speech. Magnetic Resonance in Medicine, 2019, 81, 234-246.	3.0	24
71	Deblurring for spiral realâ€ŧime MRI using convolutional neural networks. Magnetic Resonance in Medicine, 2020, 84, 3438-3452.	3.0	24
72	Quantification of Absolute Fat Mass by Magnetic Resonance Imaging: a Validation Study against Chemical Analysis. International Journal of Body Composition Research, 2011, 9, 111-122.	0.5	23

#	Article	IF	CITATIONS
73	Real-time black-blood MRI using spatial presaturation. Journal of Magnetic Resonance Imaging, 2001, 13, 807-812.	3.4	22
74	Rapid ventricular assessment using real-time interactive multislice MRI. Magnetic Resonance in Medicine, 2001, 45, 371-375.	3.0	22
75	Triggered real-time MRI and cardiac applications. Magnetic Resonance in Medicine, 2003, 49, 188-192.	3.0	22
76	Referenceless phase velocity mapping using balanced SSFP. Magnetic Resonance in Medicine, 2009, 61, 1096-1102.	3.0	22
77	Evaluation of upper airway collapsibility using realâ€ŧime MRI. Journal of Magnetic Resonance Imaging, 2016, 44, 158-167.	3.4	21
78	Systolic 3D first-pass myocardial perfusion MRI: Comparison with diastolic imaging in healthy subjects. Magnetic Resonance in Medicine, 2010, 63, 858-864.	3.0	20
79	Chemical shift encoded water–fat separation using parallel imaging and compressed sensing. Magnetic Resonance in Medicine, 2013, 69, 456-466.	3.0	20
80	Joint arterial input function and tracer kinetic parameter estimation from undersampled dynamic contrastâ€enhanced MRI using a model consistency constraint. Magnetic Resonance in Medicine, 2018, 79, 2804-2815.	3.0	20
81	Rapid quantitation of cardiovascular flow using slice-selective fourier velocity encoding with spiral readouts. Magnetic Resonance in Medicine, 2007, 57, 639-646.	3.0	19
82	Rapid measurement of renal artery blood flow with ungated spiral phase-contrast MRI. Journal of Magnetic Resonance Imaging, 2005, 21, 590-595.	3.4	18
83	Accelerated 3D MERGE carotid imaging using compressed sensing with a hidden markov tree model. Journal of Magnetic Resonance Imaging, 2012, 36, 1194-1202.	3.4	18
84	Doubleâ€gated myocardial ASL perfusion imaging is robust to heart rate variation. Magnetic Resonance in Medicine, 2017, 77, 1975-1980.	3.0	18
85	Improved velocityâ€selective labeling pulses for myocardial ASL. Magnetic Resonance in Medicine, 2020, 84, 1909-1918.	3.0	18
86	Novel 16â€channel receive coil array for accelerated upper airway MRI at 3 Tesla. Magnetic Resonance in Medicine, 2011, 65, 1711-1717.	3.0	17
87	Feasibility of throughâ€time spiral generalized autocalibrating partial parallel acquisition for low latency accelerated realâ€time MRI of speech. Magnetic Resonance in Medicine, 2017, 78, 2275-2282.	3.0	17
88	Reduced field of view MRI with rapid, <i>B</i> ₁ â€robust outer volume suppression. Magnetic Resonance in Medicine, 2012, 67, 1316-1323.	3.0	16
89	Evaluation of an independent linear model for acoustic noise on a conventional MRI scanner and implications for acoustic noise reduction. Magnetic Resonance in Medicine, 2014, 71, 1613-1620.	3.0	16
90	Test–retest repeatability of human speech biomarkers from static and real-time dynamic magnetic resonance imaging. Journal of the Acoustical Society of America, 2017, 141, 3323-3336.	1.1	16

#	Article	IF	CITATIONS
91	Demonstration of velocity selective myocardial arterial spin labeling perfusion imaging in humans. Magnetic Resonance in Medicine, 2018, 80, 272-278.	3.0	16
92	A multispeaker dataset of raw and reconstructed speech production real-time MRI video and 3D volumetric images. Scientific Data, 2021, 8, 187.	5.3	16
93	Accelerated T2*â€compensated fat fraction quantification using a joint parallel imaging and compressed sensing framework. Journal of Magnetic Resonance Imaging, 2013, 38, 1267-1275.	3.4	15
94	Model-based stability assessment of ventilatory control in overweight adolescents with obstructive sleep apnea during NREM sleep. Journal of Applied Physiology, 2016, 121, 185-197.	2.5	15
95	Real-time three-dimensional MRI for the assessment of dynamic carpal instability. PLoS ONE, 2019, 14, e0222704.	2.5	15
96	Magnetization Transfer Imaging Is Unaffected by Decreases in Renal Perfusion in Swine. Investigative Radiology, 2019, 54, 681-688.	6.2	15
97	State-of-the-Art MRI Protocol for Comprehensive Assessment of Vocal Tract Structure and Function. , 0, , .		15
98	Real-time color-flow MRI at 3 T using variable-density spiral phase contrast. Magnetic Resonance Imaging, 2008, 26, 661-666.	1.8	14
99	B compensation in 3T cardiac imaging using short 2DRF pulses. Magnetic Resonance in Medicine, 2008, 59, 441-446.	3.0	14
100	Efficient DCE-MRI Parameter and Uncertainty Estimation Using a Neural Network. IEEE Transactions on Medical Imaging, 2020, 39, 1712-1723.	8.9	14
101	Phantom Validation of DCE-MRI Magnitude and Phase-Based Vascular Input Function Measurements. Tomography, 2019, 5, 77-89.	1.8	14
102	Database of Volumetric and Real-Time Vocal Tract MRI for Speech Science. , 0, , .		14
103	<scp>MaxGIRF</scp> : Image reconstruction incorporating concomitant field and gradient impulse response function effects. Magnetic Resonance in Medicine, 2022, 88, 691-710.	3.0	14
104	Tracer kinetic models as temporal constraints during brain tumor DCEâ€MRI reconstruction. Medical Physics, 2020, 47, 37-51.	3.0	13
105	High-resolution real-time spiral MRI for guiding vascular interventions in a rabbit model at 1.5T. Journal of Magnetic Resonance Imaging, 2005, 22, 687-690.	3.4	12
106	Improved blood suppression in threeâ€dimensional (3D) fast spinâ€echo (FSE) vessel wall imaging using a combination of double inversionâ€recovery (DIR) and diffusion sensitizing gradient (DSC) preparations. Journal of Magnetic Resonance Imaging, 2010, 31, 398-405.	3.4	12
107	Minimum Field Strength Simulator for Proton Density Weighted MRI. PLoS ONE, 2016, 11, e0154711.	2.5	12
108	In vivo validation of T2―and susceptibilityâ€based S v O 2 measurements with jugular vein catheterization under hypoxia and hypercapnia. Magnetic Resonance in Medicine, 2019, 82, 2188-2198.	3.0	12

#	Article	IF	CITATIONS
109	Variable-density one-shot fourier velocity encoding. Magnetic Resonance in Medicine, 2005, 54, 645-655.	3.0	11
110	Automatic offâ€resonance correction in spiral imaging with piecewise linear autofocus. Magnetic Resonance in Medicine, 2013, 69, 82-90.	3.0	11
111	Accuracy, uncertainty, and adaptability of automatic myocardial ASL segmentation using deep CNN. Magnetic Resonance in Medicine, 2020, 83, 1863-1874.	3.0	11
112	Robust autocalibrated structured lowâ€rank EPI ghost correction. Magnetic Resonance in Medicine, 2021, 85, 3403-3419.	3.0	11
113	Improved 3D realâ€ŧime MRI of speech production. Magnetic Resonance in Medicine, 2021, 85, 3182-3195.	3.0	11
114	Rapid cardiac-output measurement with ungated spiral phase contrast. Magnetic Resonance in Medicine, 2006, 56, 432-438.	3.0	10
115	Interleaved balanced SSFP imaging: Artifact reduction using gradient waveform grouping. Journal of Magnetic Resonance Imaging, 2009, 29, 745-750.	3.4	10
116	Scan-Based Volume Animation Driven by Locally Adaptive Articulated Registrations. IEEE Transactions on Visualization and Computer Graphics, 2011, 17, 368-379.	4.4	10
117	Assessment of segmental myocardial blood flow and myocardial perfusion reserve by adenosineâ€stress myocardial arterial spin labeling perfusion imaging. Journal of Magnetic Resonance Imaging, 2017, 46, 413-420.	3.4	10
118	Realâ€ŧime multislice MRI during continuous positive airway pressure reveals upper airway response to pressure change. Journal of Magnetic Resonance Imaging, 2017, 46, 1400-1408.	3.4	10
119	Response to Letter to the Editor: "Nomenclature for realâ€ŧime magnetic resonance imaging― Magnetic Resonance in Medicine, 2019, 82, 525-526.	3.0	10
120	Regionâ€optimized virtual (ROVir) coils: Localization and/or suppression of spatial regions using sensorâ€domain beamforming. Magnetic Resonance in Medicine, 2021, 86, 197-212.	3.0	10
121	Improved coronary MR angiography using wideband steady state free precession at 3 tesla with subâ€millimeter resolution. Journal of Magnetic Resonance Imaging, 2010, 31, 1224-1229.	3.4	9
122	Non-contrast assessment of microvascular integrity using arterial spin labeled cardiovascular magnetic resonance in a porcine model of acute myocardial infarction. Journal of Cardiovascular Magnetic Resonance, 2018, 20, 45.	3.3	9
123	Intermittently tagged realâ€time MRI reveals internal tongue motion during speech production. Magnetic Resonance in Medicine, 2019, 82, 600-613.	3.0	9
124	Accelerating Dynamic Spiral MRI by Algebraic Reconstruction From Undersampled \$khbox{}t\$ Space. IEEE Transactions on Medical Imaging, 2007, 26, 917-924.	8.9	8
125	Improved 3â€Tesla cardiac cine imaging using wideband. Magnetic Resonance in Medicine, 2010, 63, 1716-1722.	3.0	8
126	Impact of (k,t) sampling on DCE MRI tracer kinetic parameter estimation in digital reference objects. Magnetic Resonance in Medicine, 2020, 83, 1625-1639.	3.0	8

#	Article	IF	CITATIONS
127	PNPLA3 Genotype, Arachidonic Acid Intake, and Unsaturated Fat Intake Influences Liver Fibrosis in Hispanic Youth with Obesity. Nutrients, 2021, 13, 1621.	4.1	8
128	Illustrating the Production of the International Phonetic Alphabet Sounds Using Fast Real-Time Magnetic Resonance Imaging. , 0, , .		8
129	Clinical Intervention to Reduce Dietary Sugar Does Not Affect Liver Fat in Latino Youth, Regardless of PNPLA3 Genotype: A Randomized Controlled Trial. Journal of Nutrition, 2022, 152, 1655-1665.	2.9	8
130	Design and use of variable flip angle schedules in transient balanced SSFP subtractive imaging. Magnetic Resonance in Medicine, 2010, 63, 537-542.	3.0	7
131	Singleâ€shot EPI for ASLâ€CMR. Magnetic Resonance in Medicine, 2020, 84, 738-750.	3.0	7
132	Real-Time Color-Flow CMR in Adults with Congenital Heart Disease. Journal of Cardiovascular Magnetic Resonance, 2006, 8, 809-815.	3.3	6
133	Prediction of myocardial signal during CINE balanced SSFP imaging. Magnetic Resonance Materials in Physics, Biology, and Medicine, 2010, 23, 85-91.	2.0	6
134	Asymmetric Synthesis 1-Substituted 2,6-Diazaspiro[3.3]heptanes through Addition of 3-Azetidinecarboxylate Anions to Davis–Ellman Imines. Organic Letters, 2019, 21, 3481-3484.	4.6	6
135	Radiofrequency transmit calibration: A multiâ€center evaluation of vendorâ€provided radiofrequency transmit mapping methods. Medical Physics, 2019, 46, 2629-2637.	3.0	6
136	Aliasing artifact reduction in spiral realâ€ŧime MRI. Magnetic Resonance in Medicine, 2021, 86, 916-925.	3.0	6
137	Accelerated 3D MRI of vocal tract shaping using compressed sensing and parallel imaging. , 2009, , .		5
138	Comparison of wideband steadyâ€state free precession and <i>T</i> ₂ â€weighted fast spin echo in spine disorder assessment at 1.5 and 3 T. Magnetic Resonance in Medicine, 2012, 68, 1527-1535.	3.0	5
139	Motion correction facilitates the automation of cardiac ASL perfusion imaging. Journal of Cardiovascular Magnetic Resonance, 2015, 17, P51.	3.3	5
140	Anisotropic fieldâ€ofâ€view support for golden angle radial imaging. Magnetic Resonance in Medicine, 2016, 76, 229-236.	3.0	5
141	SSFP and GRE phase contrast imaging using a threeâ€echo readout. Magnetic Resonance in Medicine, 2007, 58, 1288-1293.	3.0	4
142	Simple method for RF pulse measurement using gradient reversal. Magnetic Resonance in Medicine, 2018, 79, 2642-2651.	3.0	4
143	Feasibility of coronary endothelial function assessment using arterial spin labeled CMR. NMR in Biomedicine, 2020, 33, e4183.	2.8	4
144	Optimizing constrained reconstruction in magnetic resonance imaging for signal detection. Physics in Medicine and Biology, 2021, 66, 145014.	3.0	4

#	Article	IF	CITATIONS
145	Adaptive non-rigid registration of 3D knee MRI in different pose spaces. , 2008, , .		3
146	Robust autocalibrated loraks for EPI ghost correction. , 2018, 2018, 663-666.		3
147	Iterative correction of RF envelope distortion with GRATERâ€neasured waveforms. Magnetic Resonance in Medicine, 2020, 83, 188-194.	3.0	3
148	The morphology of Sella Turcica in individuals with different skeletal malocclusions – A cephalometric study. Translational Research in Anatomy, 2020, 18, 100054.	0.6	3
149	Sparse precontrast T ₁ mapping for highâ€resolution wholeâ€brain DCEâ€MRI. Magnetic Resonance in Medicine, 2021, 86, 2234-2249.	3.0	3
150	Improved Depiction of Tissue Boundaries in Vocal Tract Real-Time MRI Using Automatic Off-Resonance Correction. , 0, , .		3
151	Stabilization of alternating TR steady-state free precession sequences. Journal of Magnetic Resonance, 2008, 195, 211-218.	2.1	2
152	Arterial spin labeling CMR perfusion imaging is capable of continuously monitoring myocardial blood flow during stress. Journal of Cardiovascular Magnetic Resonance, 2015, 17, P145.	3.3	2
153	Upper Airway Narrowing during Central Apnea in Obese Adolescents. Annals of the American Thoracic Society, 2018, 15, 1465-1471.	3.2	2
154	Analysis of physiological noise in quantitative cardiac magnetic resonance. PLoS ONE, 2019, 14, e0214566.	2.5	2
155	Improved realâ€ŧime tagged MRI using REALTAC. Magnetic Resonance in Medicine, 2020, 84, 838-846.	3.0	2
156	Numerical approximation to the general kinetic model for ASL quantification. Magnetic Resonance in Medicine, 2020, 84, 2846-2857.	3.0	2
157	Liver Fat Reduction After Gastric Banding and Associations with Changes in Insulin Sensitivity and β ell Function. Obesity, 2021, 29, 1155-1163.	3.0	2
158	Pseudo Test-Retest Evaluation of Millimeter-Resolution Whole-Brain Dynamic Contrast-enhanced MRI in Patients with High-Grade Glioma. Radiology, 2021, 300, 410-420.	7.3	2
159	Effects of B 1 + Heterogeneity on Spin Echoâ€Based Liver Iron Estimates. Journal of Magnetic Resonance Imaging, 2021, , .	3.4	2
160	Myocardial blood flow is the dominant factor influencing cardiac magnetic resonance adenosine stress T2. NMR in Biomedicine, 2021, , e4643.	2.8	2
161	1138 Measurement of beat-to-beat variability of stroke volume. Journal of Cardiovascular Magnetic Resonance, 2008, 10, .	3.3	1
162	2134 Validation of the spiral Fourier velocity encoding method. Journal of Cardiovascular Magnetic Resonance, 2008, 10, .	3.3	1

#	Article	IF	CITATIONS
163	Myocardial ASL-CMR perfusion imaging with improved sensitivity using GRAPPA. Journal of Cardiovascular Magnetic Resonance, 2016, 18, P100.	3.3	1
164	Non-contrast myocardial perfusion assessment in porcine acute myocardial infarction using arterial spin labeled CMR. Journal of Cardiovascular Magnetic Resonance, 2016, 18, O7.	3.3	1
165	Resonate: Reflections and recommendations on implicit biases within the ISMRM. Journal of Magnetic Resonance Imaging, 2019, 49, 1509-1511.	3.4	1
166	Clinical Evaluation of Enamel Demineralization during Orthodontic Treatment: An in vivo Study using GC Tooth Mousse Plus. The Journal of Indian Orthodontic Society, 2014, 48, 233-238.	0.4	1
167	Cardiovascular Magnetic Resonance: Evaluation of Myocardial Function, Perfusion and Viability. , 0, , 155-191.		0
168	1091 B1+ non-uniformity in 3 T CMR: patient study. Journal of Cardiovascular Magnetic Resonance, 2008, 10, .	3.3	0
169	213 Optimally undersampled variable density spiral trajectories applied to real-time cardiac MRI at 3 Tesla. Journal of Cardiovascular Magnetic Resonance, 2008, 10, .	3.3	Ο
170	Improved scan efficiency for golden-angle radial CMR with anisotropic field-of-view. Journal of Cardiovascular Magnetic Resonance, 2016, 18, O108.	3.3	0
171	Dynamic MRI Evaluation of Moderate to Severe OSA Across the Obesity Spectrum. Chest, 2017, 152, A1085.	0.8	0
172	Prostate <scp>DCEâ€MRI</scp> with correction using an approximated analytical approach. Magnetic Resonance in Medicine, 2018, 80, 2525-2537.	3.0	0
173	Mapping of palatal bone thickness using computed tomography for placement of mini screws — A comparative study between genders, adolescents and adults. Orthodontic Waves, 2019, 78, 18-25.	0.2	0
174	lschemic Heart Disease: Myocardial Perfusion Imaging. Fundamental and Clinical Cardiology, 2006, , 179-194.	0.0	0
175	Sensitivity of Quantitative RT-MRI Metrics of Vocal Tract Dynamics to Image Reconstruction Settings. , 0, , .		0
176	Perceived Dark Rim Artifact in First-Pass Myocardial Perfusion Magnetic Resonance Imaging Due to Visual Illusion. Korean Journal of Radiology, 2020, 21, 462.	3.4	0
177	Creating an animatable 3D volume hand model from in vivo MRI. Studies in Health Technology and Informatics, 2008, 132, 402-7.	0.3	Ο